Friday, July 31, 1998
IRON METEORITES
10:15 a.m. Ussher Theatre

Chairs: V. Buchwald
A. Kracher

Herzog G. F.* Schnabel C. Xue S. Masarik J. Cresswell R. G. di Tada M. L. Liu K. Fifield L. K.
Nickel-59 in Canyon Diablo Spheroids and Meteorites

Honda M.* Nagai H. Kobayashi T.
Cosmogenic Radionuclides in Large Iron Meteorites

Maruoka T.* Matsuda J. Kurat G.
Xenon-HL in the Magura IAB Iron Meteorite

Goldstein J. I.* Reisner R. J. Rancourt D. G. Lagarec K. Scorzelli R. B.
The Santa Catharina Meteorite: A Cloudy Zone Microstructure Consisting of a Fine Intergrowth of Tetrataenite and Antitaenite

Chabot N. L.* Drake M. J.
Examining Crystallization Scenarios for Magmatic Iron Meteorites with a Mixing Model

Ulff-Møller F.*
The Role of Solid-state Diffusion of Phosphorus During Core Solidification in Iron Meteorite Parent Bodies

Kracher A.* Gramstad S. D. Kurat G.
Soroti and the Origin of Sulfide-rich Meteorites

Jones J. H.*
Uncertainties in Modeling Core Formation

* Denotes Speaker

NICKEL-59 IN CANYON DIABLO SPHEROIDS AND METEORITES. G. F. Herzog[1], C. Schnabel[1], S. Xue[2], J. Masarik[3], R. G. Cresswell[4], M. L. di Tada[4], K. Liu[4], and L. K. Fifield[4], [1]Department of Chemistry., Rutgers University, Piscataway NJ 08854-8087, USA (herzog@rutchem.rutgers.edu), [2]Graduate School of Oceanography, University of Rhode Island, Narragansett RI 02882-1197, USA, [3]Department of Nuclear Physics, Komensky University, Mlynska dolina F/1, SSSSK-842 15 Bratislava, Slovakia, [4]Department of Nuclear Physics, Research School of Physical Science and Engineering, Australian National University, Canberra, ACT 0200, Australia (keith.fifield@anu.edu.au).

Introduction: Canyon Diablo spheroids formed by the rapid quenching of melted projectile [1]. Just as noble gas data first indicated the portion of the projectile that fragmented to produce meteorites -- the outermost meter or so [2] -- so the ^{59}Ni contents of spheroids can help identify the portion that melted [3]. Because the spheroids underwent both heating and oxidation, other commonly measured cosmogenic nuclides such as ^{21}Ne, ^{10}Be, and ^{26}Al are inappropriate for this purpose. Our approach has three parts: to measure ^{59}Ni ($T_{1/2}$=76 ka) in various spheroid samples; to measure ^{59}Ni in Canyon Diablo meteorite specimens for comparison; and to carry out modeling calculations of ^{59}Ni production to aid in interpretation.

Experimental methods: Samples analyzed included a Ni standard kindly supplied by J. Klein; the Canyon Diablo meteorite specimen 4340; and a 122-mg collection of Canyon Diablo spheroids. The spheroids had an average mass of 10 mg and were cleaned by repeated etching with 5% HF, washing, and magnetic raking. For the measurement of ^{59}Ni by accelerator mass spectrometry we enhanced the methods of [4] by adding a velocity filter.

Results & Discussion: Results of the measurements are as follows: (sample, ^{59}Ni/Ni÷0.68=^{59}Ni/^{58}Ni [10^{-12} atom/atom]): (Standard, 37.7±5%); (Canyon Diablo 4340, 9.5± 15%); (Canyon Diablo spheroids V-3, 1.1± 25%). The results for the standard agree well with those reported previously [4]. Figure 1 shows the ^{59}Ni/^{58}Ni ratios of the spheroids corrected for a terrestrial age of 50 ka [6] and plotted at depths inferred from the calculated production rate curve (i.e., *not* at independently determined depths). The ^{59}Ni/^{58}Ni ratio for the spheroid sample V-3, agrees well with that of sample SC-P but is lower than that of SC-O (Fig. 1) [3].

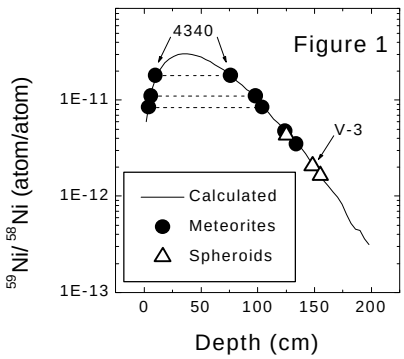

Published ^{59}Ni/^{58}Ni ratios for Canyon Diablo meteorites range from ~2-7 $\times 10^{-12}$ [5]. All these values are consistent with depths of less than 140 cm (Fig. 1). For three of the meteorites the ^{59}Ni activities allow two depth assignments (dashed tie-lines). Most Canyon Diablo specimens, however, have ^{10}Be, ^{26}Al, and ^{36}Cl activities that imply depths well below the surface [7]. For this reason, we favor the higher depth estimates.

The range of ^{59}Ni contents in the meteorite specimens corresponds to a range of depths of ~40 cm (320 g/cm^2), which is comparable to the range inferred from the ^{10}Be, ^{26}Al, and ^{36}Cl activities [7]. The absolute ^{59}Ni-based depth of 76 cm for Canyon Diablo 4340 disagrees with depths of ~48 cm based on ^{10}Be, ^{26}Al and ^{36}Cl [7]. Similarly, the ^{59}Ni-based depths inferred for various Canyon Diablo samples reported in the literature are systematically larger than those inferred for the set of samples studied by [7]. Three possible reasons for these discrepancies are measurement errors; overestimates in the ^{59}Ni production rate calculation; and an incorrect terrestrial age. A terrestrial age of 100 ka would reconcile the depth estimates.

Even allowing for a factor-of-two error in the terrestrial age, however, the ^{59}Ni contents of the spheroids are well below values expected at the projectile surface and generally lower than those measured in meteorites. These observations strongly suggest that the spheroids came from larger depths in the impactor than did the meteorites and add to the arguments against stripping and ablation as important mechanisms for spheroid formation [8].

References: [1] Blau P. J. et al. (1973) *JGR, 78,* 363-374. [2] Heymann D. et al. (1966) *JGR, 71,* 619–641. [3] Klein J. et al. (1995) *LPS XXVI,* 763–764. [4] Paul M. et al. (1993) *Nucl. Instrum. Meth., B83,* 275–283. [5] Honda M. and Arnold J. R. (1967) *Handb. Phys. 46,* 613-632; Kaye J. H. (1962) Progress Report for U.S. Atom. Energy Comm. Contract AT(30-1)-844. [6] Nishiizumi K. et al. (1991) *GCA, 55,* 2699–2703; Phillips F. M. et al. *GCA, 55,* 2695–2698; Sutton S. R. (1985) *JGR, 90,* 3690–3700. [7] Michlovich E. S. et al. (1994) *JGR Planets, 99,* 23187–23194. [8] Nininger H. H. (1956) *Arizona's Meteorite Crater,* World Press, Denver, Colorado. 101–105.

COSMOGENIC RADIONUCLIDES IN LARGE IRON METEORITES. M. Honda, H. Nagai, and T. Kobayashi, Nihon University, Department of Chemistry, Sakura-josui, Setgaya, Tokyo 156, Japan (BZG13477@niftyserve.or.jp; hnagai@chs.nihon-u.ac.jp; tkoba@chs.nihon-u.ac.jp).

Introduction: Long-lived cosmogenic nuclides have been determined in extremely large irons. To systematize these data, however, we have to select useful sets of determinations. The following considerations lead to systematic treatment[1]: (1) Meteoroids must be large enough so that practical 2π geometry model is applied in general. (2) The data are obtained from simultaneous determinations for higher and lower energy products in a specimen. This makes possible to visualize the shielding of steady state irradiation. (3) A dataset of certain nuclide in various fragments are also useful. There may be three categories; those from near surface, those of interior, and information from center can be compared as a function of shielding. (4) Stable nuclide data are not always useful for direct comparisons, because possible complex irradiation histories may give interference to interpretations.

The meteorites suitable for this study are Campo del Cielo, Canyon Diablo, Gibeon, Odessa, Sikhote-Alin, and others. Besides irons, metal phase of the Brenham pallasite, could be treated approximately in the same group [2]. All data are expected to inform us a unified mechanism in the irradiation history. The radionuclides ^{53}Mn, ^{10}Be, ^{26}Al, ^{36}Cl, ^{39}Ar, and ^{41}Ca can be determined conveniently. When shielding conditions are specified, other lower energy products will also be useful.

Experiment: Useful sets of data were collected from the simultaneous determinations for ^{53}Mn as a low energy product, ^{10}Be and ^{26}Al as high-energy products, in some fragments that have been offered from various sources. Normally one gram size samples are taken, and the mixture of 0.1–2-mg carriers is added. After wet chemical separations, AMS method for ^{10}Be and ^{26}Al, and neutron activation for ^{53}Mn were applied.

Results: On the whole, a common feature can be pointed out throughout all irons and the products in the simple functions of depths. In fact, the very surface material in space cannot be available similar to other meteorites. In the near surface fragments, under the lower shielding, 250–300 dpm ^{53}Mn/kg are found, and they are the highest among the fragments. At the same time, for ^{10}Be, 2–2.5, for ^{26}Al, 1.5–2 dpm/kg are found: they are about 1/2 of the highest contents inside smaller irons. It is not rare to have these specimens from many irons. In Sikhote Alin, 320 dpm ^{53}Mn/kg have been observed, which is higher than the maximum GCR productions in the lunar regolith, 220 dpm/kgFe, at 50–100 g/cm^2. Perhaps that difference can be attributed to those of bulk compositions, 12% Fe or lower are in lunar soil. In Canyon Diablo and Odessa, however, 250–200 dpm/kg are found in their higher groups[3].

In intermediate regions, various degrees of productions are observed. The variation range is extensive, 103 or more, between 100 and 1200 g/cm^2 in a single object. Because of the wide range, some small empirical uncertainties may not cause serious problems. The data are plotted as function of shielding, conveniently with production rate ratios of high and low energy products, such as P(^{4}He)/P(^{21}Ne). Actually they can be derived indirectly from P(^{53}Mn)/P(^{26}Al) and others. Because 2π geometry model can be applied for these large objects, exponential profiles can be illustrated applying depths approximately extrapolated from lunar core sample data.

Near the center of Campo del Cielo and Nantan, no reliable data are available simply because of extremely low contents. They are E-3 or lower of the surface values beyond current detection limits. Actually the deepest fragments of Brenham seem to indicate the situation closer to 4π.

References: [1] Honda M. (1988) *Meteoritics, 23*, 3. [2]Honda M. et al. (1998) *Cosmogenic Nuclides in Brenham Pallasite,* in preparation. [3]Nishiizumi K. (1987) *Nucl. Tracks Radiat. Meas., 13*, 209.

XENON-HL IN THE MAGURA IAB IRON METEORITE. T. Maruoka[1], J. Matsuda[1], and G. Kurat [2], [1]Department of Earth and Space Science, Graduate School of Science, Osaka University, Toyonaka, Osaka 560-0043, Japan (terry@ess.sci.osaka-u.ac.jp), [2]Naturhistoriches Museum, Postfach 417, A-1014 Vienna, Austria.

IAB iron meteorites are considered to be of non-magmatic origin because their trace element abundances cannot be explained by simple partitioning between solid and liquid metal. Although several models have been proposed to explain these anomalous elemental abundances (e.g., Kelly and Larimer [1]; Choi et al. [2]), the origin of IAB irons is still not well understood. In order to find additional constraints for the formation of IAB irons, we analyzed the elemental and isotopic compositions of noble gases in the Magura IAB iron meteorite.

We analyzed two bulk metals of the Magura iron which contained visible graphite inclusions. The stepwise heating technique (800°, 1200°, and 1600°C) was applied for the gas extraction. The trapped Xe of the 800°C fractions is dominated by El Taco Xe [3], whereas Xe of the high temperature fractions is a mixture of El Taco Xe and Q-Xe. Such a relationship between the extraction temperature and the isotopic compositions of trapped gases was also observed in a graphite nodule of the Bohumilitz IAB iron [4].

The 800°C fraction of the Magura metal contains a small amount (4% of ^{132}Xe, i.e., 3×10^{-13}cm^{3}STP/g) of Xe-HL. Xenon-HL is a typical trapped noble gas component of pre-solar diamonds where it is present in large amounts (about 10^{-7} cm^{3}STP/g ^{132}Xe-HL [5]). This component is not present in the high temperature gas fractions (1200° and 1600°C). This observation appears to be inconsistent with the thermal characteristics of pre-solar diamonds which release most of the Xe-HL component between 1200° and 1600°C [5]. However, the analyses by Huss and Lewis [5] also indicate the presence of a Xe-HL sub-component which is released between 700° and 1100°C and which is present only in the diamonds from the most primitive chondrites such as Orgueil (CI) and Semarkona (LL3.0). Therefore, the presence of a Xe-HL component only in the 800°C fractions of the Magura IAB iron metal may suggest that the source matter of IAB irons is somehow related to that of the most primitive chondrites.

Acknowledgments: This study was supported in part by Research Fellowship of the Japan Society for the Promotion of Science for Young Scientists.

References: [1] Kelly W. R. and Larimer J. W. (1977) *GCA, 41*, 93–111. [2] Choi B. et al. (1995) *GCA, 59*, 593–612. [3] Mathew K. J. and Begemann F. (1995) *GCA, 59*, 4729–4746. [4] Maruoka T. et al. (1998) *LPSC XXIX*. [5] Huss G. R. and Lewis R. S. (1994) *GCA, 29*, 811–829.

THE SANTA CATHARINA METEORITE: A CLOUDY ZONE MICROSTRUCTURE CONSISTING OF A FINE INTERGROWTH OF TETRATAENITE AND ANTITAENITE. J. I. Goldstein[1], R. J. Reisner[1], D. G. Rancourt[2], K. Lagarec[2], and R. B. Scorzelli[3], [1]College of Engineering, University of Massachusetts, 125 Marston Hall, Amherst MA 01003, USA, [2]Department of Physics, University of Ottawa, Ontario, Canada K1N 6N5, [3]Centro Brasileiro de Pesquisas Físicas, Rua Xavier Sigaud 150, 22290-180 Rio de Janeiro, Brazil (scorza@cat.cbpf.br).

The Santa Catharina meteorite has attracted attention from researchers because of its nominal bulk Ni content near the Invar composition (36wt% Ni, 64 wt% Fe). The interest in this meteorite has been further increased by the discovery of the mineral tetrataenite, i.e., tetragonal ordered FeNi. Tetrataenite was first observed in Santa Catharina by Danon et al. [1] using Mossbauer spectroscopy. About 50% of the meteorite was composed of this phase together with a high percentage of an atomically disordered gamma FeNi phase, with lower Ni content. This low-Ni phase is always observed microstructurally in close association with tetrataenite. The low-Ni phase was reported by Rancourt and Scorzelli [2] to be a low-moment gamma Fe-Ni phase. This new mineral was called antitaenite, based on the antiferromagnetism of its synthetic analogues and to stress its difference with ordinary (high-moment) taenite. The association of these two phases (tetrataenite and antitaenite) has also been observed by Mossbauer spectroscopy in other meteorites. Detailed investigations of the microstructural features of the metal in Santa Catharina have been carried out by Zhang et al. [3] and Yang and Goldstein [4] using a variety of electron optical techniques in different Santa Catharina samples with different bulk Ni values and different degrees of oxidation. The metallic regions of Santa Catharina have a microstructure containing cloudy zone, and intimate mixture of an island phase of tetrataenite in a honeycomb matrix phase.

Combined bulk (X-ray diffraction, magnetometry, Mossbauer spectroscopy) and microscopic measurements (high resolution SEM, EPMA) were obtained on a nonoxidized Santa Catharina sample. The metal phase contained 33.0 $\pm$ 0.3 wt% Ni, 66.2 $\pm$ 0.5 wt% Fe, 0.54 $\pm$ 0.03 wt% Co and 0.01 to 0.43 wt% P. The size of the island phase (tetrataenite) is 20 to 40 nm. The honeycomb matrix phase of the cloudy zone microstructure is interpreted to be the low-spin phase (antitaenite) observed by Mossbauer spectroscopy. The calculated composition of antitaenite is 15$\pm$ 5 wt% Ni. The cloudy zone microstructure itself was most likely formed in high temperature taenite by a spinodal decomposition below about 350^0 C during slow cooling. The size of the island phase indicates a maximum cooling rate of approximately 50 to 250^0 C per million years using the cooling rate method of Yang et al., [5]. This cooling rate is very high for the iron meteorites and comparable to that of the IVA irons. Oxidation of Santa Catharina metal is argued to have resulted from atmospheric exposure and is probably not an intrinsic feature of pristine samples.

Acknowledgments: Supported in part by NASA grant NAGW-4514 to J. I. Goldstein. D.G.R. and K.L. acknowledge financial support from the NSERC of Canada. R. B. Scorzelli is grateful to CNPq for financial support.

References: [1] Danon J. et al. (1978) *C. R. Acad. Sci. Paris, B-199*, 287. [2] Rancourt D. G.and Scorzelli R. B. (1995) *J. Magn. Magn. Mater., 150*, 30. [3] Zhang J. et al. (1990) *Meteoritics & Planet. Sci., 25*, 167. [4] Yang C. W. and Goldstein J. I. (1997) *The Invar Effect, The Minerals*, p. 137, Metals & Materials Society. [5] Yang C. W. et al. (1997) Meteoritics & Planet. Sci., 32, 423.

EXAMINING CRYSTALLIZATION SCENARIOS FOR MAGMATIC IRON METEORITES WITH A MIXING MODEL. N. L. Chabot and M. J. Drake, Lunar and Planetary Laboratory, University of Arizona, Tucson AZ, 85721 (chabot@lpl.arizona.edu).

Magmatic Fe meteorites, when plotted by group on element vs. element diagrams, display well-defined trends which are usually attributed to the solidification of once molten metallic cores of asteroid-sized bodies [1]. Simple fractional crystallization calculations appear to reproduce elemental trends observed in the IIIAB iron meteorite group when these trends are plotted vs. Ni, as is traditionally done. However, when the elemental trends are examined vs. another element, such as Ge vs. Ir, simple fractional crystallization fails to match a significant portion of the trend, specifically the meteorites formed during the final stages of crystallization. A mixing model, which allowed the crystallizing liquid to develop inhomogenieties due to incomplete mixing in the molten core, was able to fit the IIIAB Ge vs. Ir trend [2].

However, this previous mixing model was not a closed system; in order to simulate inhomogenieties in the liquid, additional amounts of liquid of different compositions were added throughout the crystallization calculations. We have kept the fundamental concept of this previous model, that the molten core does not remain homogeneous as solid metal crystallizes, but have now developed a closed system model of core crystallization.

Figure 1 illustrates the parameters of the new mixing model. The molten core is considered to be composed of two reservoirs, *Zone 1* and *Zone 2*. *Zone 1* is the metallic liquid which is actively involved in the crystallization process, and whose composition consequently changes because of the crystallization of solid metal. *Zone 2* is the remaining metallic liquid which is too far from the actively crystallizing solid to be affected by the crystallization process. *Zone 1* and *Zone 2* are allowed to interact with each other through the model parameters *move* and *mix*, which are rates of processes relative to the rate of crystallization. As illustrated in Fig.1, *mix* is a simple swapping of liquid and will change the compositions of both zones; if *mix* is set to a high value, the rate of mixing is fast compared to the rate of crystallization and the resulting model calculations are identical to simple fractional crystallization. The parameter *move* controls the relative sizes of *Zone 1* and *Zone 2*. Unlike with the parameter *mix*, the process of *move* only changes the composition of one of the zones, since *move* is an incorporation of liquid which was previously in the other zone.

The actual calculations in the model are carried out as equilibrium crystallization in about 10,000 steps. Experimentally determined solid metal/liquid metal partition coefficients, which vary as a function of the S and P concentration in the metallic liquid, are used to calculate the resulting solid metal elemental trends which crystallize from *Zone 1* [3–5]. Between each crystallization step, the parameters *mix* and *move* change the compositions of the two zones of liquid.

Four distinctly different crystallization scenarios involving mixing for the core of an asteroid-sized body are considered. These scenarios range from outward crystallization with a small core/mantle boundary layer to inward crystallization with a constant sized zone of crystallizing liquid. All four scenarios are found to reproduce the Ge vs. Ir IIIAB elemental trend which simple fractional crystallization could not. Thus, mixing can effectively buffer element concentrations and explain the late stage crystallizing IIIAB Fe meteorites.

Acknowledgments: Research supported by NASA grants NGT-550132 and NAG5-4084.

References: [1] Scott E. R. D. (1972) *GCA, 36*, 1205–1236. [2] Chabot N. L. and Drake M. J. (1996) *Meteorit. Planet. Sci., 31*, A26–A27. [3] Jones J. H. and Malvin D. J. (1990) *Metall. Trans., 21B*, 697–706. [4] Haack H. and Scott E. R. D. (1993) *GCA, 57*, 3457–3472. [5] Chabot N. L. and Drake M. J. (1997) *Meteorit. Planet Sci., 32*, 637–645.

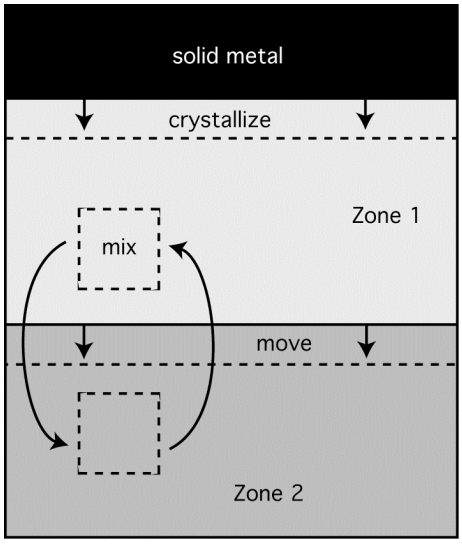

Fig.1. Illustration of the two reservoirs of the molten core, *Zone 1* and *Zone 2*, and the model parameters *mix* and *move*.

THE ROLE OF SOLID-STATE DIFFUSION OF PHOSPHORUS DURING CORE SOLIDIFICATION IN IRON METEORITE PARENT BODIES. Finn Ulff-Møller, Institute of Geophysics and Planetary Physics, University of California, Los Angeles CA 90095-1567, USA.

Diffusion is usually assumed to be negligible in the solid metal crystallizing in asteroidal cores - a basic assumption for fractional crystallization models. This assumption holds well for metallic trace elements with comparatively low diffussivities [1] and fairly well for P which diffuses more than an order of magnitude faster than the metallic trace elements [1,2]. The actual flux of P is a function of the magnitude of the chemical gradients formed during solidification and of the thermal history. Typically, low P gradients will form during the early stages of crystallization but later, two processes are capable of creating stronger gradients. Liquids with initial S/P ratios below 0.1 can evolve to high P contents in the homogeneous state, whereas liquids with higher initial S/P ratios eventually will reach the liquid immiscibility field in the Fe-P-S system [3] and separate into a sulfide liquid and a metal liquid. Particularly in the case of liquid immiscibility there is a rapid enrichment of P in the metal liquid. In both cases this is where the effects of diffusion in solid metal may play the strongest role.

Numerical calculations of the diffusion of P in the crystallizing metal was done by assuming one-dimensional diffusion and a constant (solid/liquid) distribution coefficient for P of 0.1. A constant cooling rate of the order of 25 K/Ma was estimated from a solidification interval of about 500 K (for low initial amounts of S and P) and the 20 Ma time interval of formation of the magmatic iron meteorites from Ag-Pd isotope systematics [4].

For cells of the sizes of 1000 m and 100 m, diffusion changed the P content in the first metal that crystallized by factors of 1.02 and 1.15, respectively. These changes occur mainly in the first 300 K of the solidification interval and are of the same order of magnitude as the uncertainty of the estimated P contents in individual iron meteorites, suggesting that diffusion in the low-gradient regime is negligible. However, for shorter diffusion distances and highly evolved liquids that create stronger gradients, an increasing amount of P diffuses into the solid metal.

For a liquid that evolves in the homogeneous state, back-diffusion of P has a modest effect on trace element fractionation because of the much weaker effect of P on trace element partitioning than that of S[5]. However, in the case of liquid immiscibility, the quantity of metal liquid is being controlled by the amount of P and this quantity becomes small relative to the quantity of sulfide liquid at late stages of the evolution. In this case, back-diffusion will change the size of the reservoir which has a large effect on the behavior of the siderophile elements.

REFERENCES: [1] Dean and Goldstein J. I. (1986) Metall. Trans. **17A,** 1131-1138. Narayan and Goldstein (1983) Metall. Trans. **14A,** 2437-2439. [2] Heyward and Goldstein (1973) Metall. Trans. **4,** 2335-2342. [3] Ulff-Møller (1998) MAPS **33**, 207-220. [4] Chen and Wasserburg (1990) GCA **54,** 1729-1743. [5] Jones and Malvin (1990) Metall. Trans. **21B,** 697-706.

SOROTI AND THE ORIGIN OF SULFIDE-RICH METEORITES. A. Kracher[1], S. D. Gramstad[1] and G. Kurat[2], [1]Iowa State University, 253 Science I, Ames, IA 50011-3212, (akracher@iastate.edu), [2]Naturhistorisches Museum Wien.

Introduction: Sulfide-rich meteorites are differentiated meteorites whose sulfide abundance is higher than that of chondrites. Since meteorite parent bodies are presumed to have chondritic bulk compositions, and typical differentiated meteorites contain less sulfide than chondrites, the scarcity of sulfide-rich meteorites is puzzling.

Most S-rich meteorites are compositionally distinct from known meteorite groups. However, since most cores parental to known iron meteorite groups are expected to produce S-rich material, it is unlikely that none of these S-rich samples come from a body sampled by other meteorites.

Parent Materials: Sulfide-rich regions may form on asteroids by a number of processes, e.g., (a) as residual melt from core formation, (b) as partial melt, (c) as a result of shock melting, and (d) due to liquid immiscibility. Any of these processes may result in a metal/sulfide assemblage whose composition is quite different from other materials in the same asteroid. It may thus be difficult to recognize relationships between known meteorite groups and sulfide-rich meteorites. Identifying possible relationships between S-rich "oddballs" and other meteorites requires both a careful study of the S-rich samples and improved quantitative models of their formation.

Soroti: We have studied the most sulfide-rich meteorite known, Soroti. It consists mostly of troilite and nickel-iron with a grain size of several cm. The (Fe,Ni) matrix contains numerous small inclusions of sphalerite, commonly associated with troilite or chromite. The latter is characterized by unusually high (>3%) ZnO, and highly variable MnO: from 0.26% (chromite in metal) to 7.1% (chromite in contact with troilite). Phosphate inclusions contain F-apatite, buchwaldite, and at least two other phosphates. Very minor amounts of ferroan alabandite, djerfisherite, native Cu, and pentlandite are found in troilite.

The high sulfide abundance of Soroti and the low Ir content of its metal phase suggest formation from residual melt after extensive fractional crystallization. Reasonable models of this process may reveal possible associations with known iron meteorite groups, although there are too many uncertainties to conclusively establish any such relationship.

The behavior of minor elements is consistent with the proposed origin. Chromium tends to become enriched in S-rich melts, and both P and Cr scavenge available O to form phosphates and chromite with falling temperature. How Zn and Mn react in this environment is unknown, but assuming a behavior similar to that of Cr is reasonable.

LEW86211: Although the sulfur content of LEW86211 is nearly as high as that of Soroti, the two meteorites are different in almost every conceivable way: the texture of LEW86211 is almost 1000× finer, its Ge and Ir contents are much higher, and Ni is lower. Also, the mineralogy of minor phases appears to be quite different, although we have not yet studied it in detail. Chemistry and texture indicate rapid cooling, which is more consistent with a local formation process such as impact.

UNCERTAINTIES IN MODELING CORE FORMATION. J. H. Jones, SN2, NASA/Johnson Space Center, Houston TX 77058 (john.h.jones1@jsc.nasa.gov).

Introduction: Recent advances have permitted core formation to be modeled more realistically, simultaneously taking several intensive variables into account [1]. Using the convergence of models for five different siderophile elements (Co, Ni, Mo, P, W), Righter et al. [1] concluded that terrestrial core formation occurred *via* equilibrium between a silicate liquid and a metallic liquid as the Earth passed through a magma ocean stage. The separation of metal and silicate is believed to have occurred at 270 kbar, ~1900°C, and a $\log fo_2$ of IW-0.15. In the model of [1], the metallic liquid contained 15 mole% S and the bulk Earth contained CI abundances of siderophile elements. Strangely, this model predicts conditions that would be deeply subsolidus in the present-day mantle, even though the premise is that the mantle was molten [1].

Models of Core Formation: There are several potential problems with the method of [1]. One important issue is that [1] did not separate experiments containing C from those that did not. Typically only high-pressure experiments contain C. Therefore, effects due to C may possibly have been attributed to pressure in multivariate regressions. Consequently, I have regressed literature partitioning data from C-free experiments for Ni, Co, and W. In Table 1 R&D refers to regressions of [1] and JJ refers to the present work. Primed models denote those with experiments containing sulfur. Of especial concern is the difference between the results of this effort and that of [1] in terms of the *signs* of the regression parameters (Table 1). Further, some simplifications are apparently possible: In the nonmetal-free system, D_{Ni} depends only on fo_2 and pressure; D_{Co} depends only on fo_2 and temperature; and D_W depends only on fo_2 and silicate composition. Addition of S to the system (X_S) typically increases the required complexity of the regression. However, it is gratifying that the coefficients for the P/T and $\ln(1-2\alpha X_S)$ terms of my Ni´ model are essentially identical to those of [2] and [3], respectively.

Application to the Earth: Under the constraints of whole-Earth melting and $X_S \approx 0.2$ in the core, the equations for W, Ni, and Co are sufficient to calculate a set of self-consistent conditions for core formation, assuming that bulk Earth Ni/Fe, Co/Fe, and W/La ratios are chondritic. The results are: $\log fo_2$= IW-1.75, T= 3700°C, and P= 110 kbar. These results are sufficiently different from those of [1] that the modern terrestrial mantle would be entirely molten under these conditions. However, at this juncture strong conclusions are premature, and scenarios without a magma ocean should still be considered [4].

References: [1] Righter K. et al. (1997) *Phys. Earth. Planet. Int., 100,* 115–134. [2] Li J. and Agee C. B. (1996) *Nature, 381,* 686–689. [3] Jones J. H. and Malvin D.J. (1990) *Metallurg. Trans., 21B,* 697–706. [4] Jones J. H. (1996) *Philos. Trans. R. Soc. London, 354A,* 1481–1494.

lnD(metal*/silicate liquid)
Regression Coefficient Summary

lnD	$\ln fo_2$ or ln(•IW)	P/T (kbar/K)	1/T (K^{-1})	#F(nbo/t)
Ni´ — R&D	-0.513	43.5	-20521	-0.327
Ni — JJ	-0.443	-79.4	—	—
Ni´— JJ	-0.452	-25.1	10440	—
W´ — R&D	-1.10	144	-97150	-0.770
W — JJ	-1.40	—	—	0.801
W´— JJ	—	—	—	—
Co´ — R&D	-0.508	56.07	-26892	-0.186
Co — JJ	-0.484	—	8457	—
Co´— JJ	-0.482	—	8368	—

lnD (con't)	$F(X_S)$	Const.	+N	Error	r^2
Ni´ — R&D	-3.09	7.016	102	0.45	0.89
Ni — JJ	—	7.118	59	0.46	0.89
Ni´ — JJ	-0.314	0.263	65	0.43	0.92
W´ — R&D	-4.94	31.4	48	0.88	0.88
W — JJ	—	-1.816	27	0.94	0.87
W´— JJ	NA	—	—	—	—
Co´ — R&D	-1.698	8.366	31	0.39	0.97
Co — JJ	—	-1.164	32	0.50	0.89
Co´— JJ	-0.209	-1.108	38	0.47	0.89

*Equations of [1] are for liquid metal; my regressions do not discriminate between solid and liquid metal; #F(nbo/t) is the functional form parameterizing the effect of silicate liquid composition. R&D use nbo/t (Mysen, 1983); I use $\ln\{[4-(nbo/t)]/(nbo/t)\}$. Differences between these methods are small. $R&D use $\ln(1-X_S)$; I use $\ln(1-2.18\ X_S)$ [3]. These two functions are only colinear at small values of X_S. +Number of experiments regressed. NA, data not available.